Pure Appl. Chem., Vol. 84, No. 4, pp. 879–891, 2012.
http://dx.doi.org/10.1351/PAC-CON-11-09-25

Double-stranded polymeric ladderphanes*

Tien-Yau Luh

Department of Chemistry, National Taiwan University, Taipei 106, Taiwan

Abstract: Double-stranded polymeric ladderphanes are obtained by ring-opening metathesis polymerization (ROMP) of bisnorbornene derivatives by the first generation of Grubbs catalyst (G-I). A range of two- and three-dimensional organic and organometallic linkers are used to connect two norbornene units. The structures of these double-stranded polymers are proved by spectroscopic means and scanning tunneling microscopic (STM) images. Hydrolytic cleavages of these ladderphanes give the corresponding single-stranded polymers with the same degree of polymerization and polydispersity as those of the double-stranded counterparts. Helical polymeric ladderphanes are also synthesized similarly when chiral linkers are used. Strong intereactions between adjacent linkers have been revealed by their physical properties in these polymers. Chemical modification of ladderphanes is achieved by bis-dihydroxylation, diimide reduction of double bonds, and electrochemical oxidation of linkers. Unsymmetrical ladderphanes with well-defined lengths and narrow dispersity are also obtained by replication and by sequential polymerization.

Keywords: double-stranded ladderphanes; olefin metathesis; organometallic chemistry; polymerization; polynorobornenes; replication; scanning tunneling microscopy; tacticity.

INTRODUCTION

A polymeric ladderphane is defined as multiple layers of cyclophanes where the tethers are part of the polymeric backbones [1]. It can also be considered as an array of aromatic rings or related species aligned face-to-face along the longitudinal axis of the polymer (Fig. 1). It is generally believed that the charge-carrier mobility in organic semiconductors is closely related to π–π interactions between adjacent aromatic chromophores [2–5]. Cofacial long-range π-stacking toward highly ordered layer arrangement of aromatic rings, in general, yields strong electronic coupling between these π-conjugated systems, resulting in high charge mobility [2–5]. However, large-area processing with such cofacial alignment for device applications is not trivial. It is envisaged that supramolecular architectures may offer an alternative possibility to assemble these planar π-systems arranged cofacially. In this account, we summarize the recent advances on the design, synthesis, characterization, and photophysical properties as well as aggregation patterns of these highly symmetric double-stranded ladderphanes.

Pure Appl. Chem.* **84, 861–1112 (2012). A collection of invited papers based on presentations at the 14th International Symposium on Novel Aromatic Compounds (ISNA-14), Eugene, OR, USA, 24–29 July 2011.

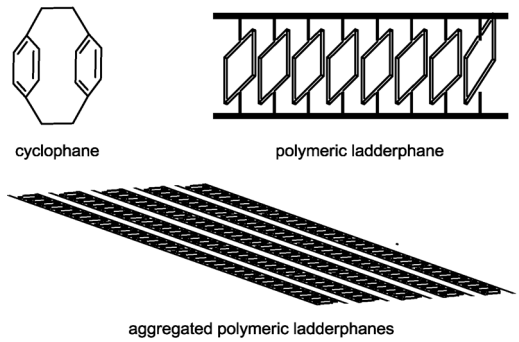

Fig. 1 Structures of a cyclophane, a polymeric ladderphane, and its aggregated form.

BACKGROUND

We recently reported the synthesis of first double-stranded polybisnorbornenes **2** from the corresponding bisnorbornene monomer having a ferrocene linker **1** by ring-opening metathesis polymerization (ROMP) using the first generation of the Grubbs catalyst (G-I) **3** (Scheme 1) [6–8]. The ferrocene linkers in **1** form a linear array with the Fe–Fe distance around 5.5 Å. This distance turns out to be the spacing occupied by each of the monomeric vinylcyclopentane units in **2** [9,10]. The adjacent ferrocene groups may interact strongly with each other as revealed by the electrochemical and magnetic studies [11]. The presence of the *endo*-fused *N*-arylpyrrolidine moieties in the linker between two norbornene units in **1** is crucial to control the isotactic stereochemistry and trans double-bond selectivity in the ROMP process under these conditions [6–13]. Interactions between these pending aryl groups might take place during the course of the polymerization and would be responsible for the stereoselectivity of the polymerization reaction [12].

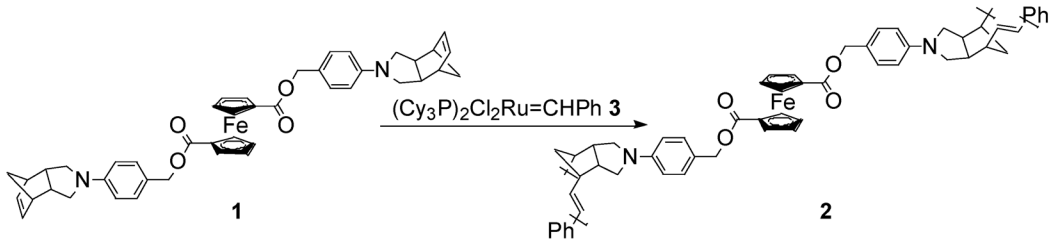

Scheme 1

Unsymmetrical polybisnorbornene **7** is obtained by the ROMP of **6**, which is prepared by the esterification of the single-stranded polynorbornene **4** and monomer **5**. Base-promoted hydrolysis of **7** followed by esterification gives the corresponding daughter polymer **8** (Scheme 2). This protocol can be considered as the replication of **4** to furnish **8** [14].

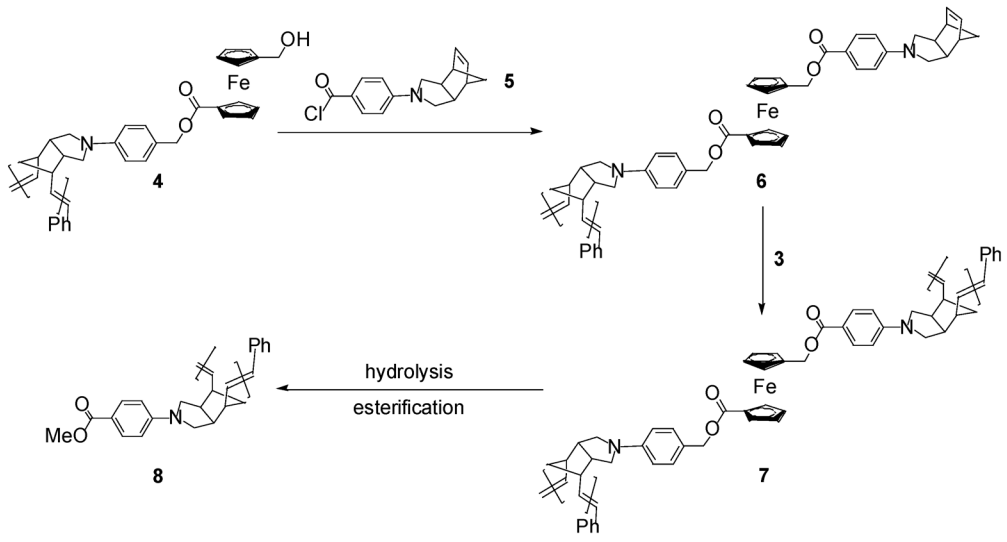

Scheme 2

Since the G-I catalyst is used and the reaction is quenched by ethyl vinyl ether, styrene and vinyl end groups are present in these polymers. Polymers **2** and **7** assemble nicely on the highly ordered pyrolytic graphite (HOPG) surface to form a two-dimensional array (Figs. 2a–c) [14,15]. Although the average length of **7** is about 15 nm, the polymers tend to form aggregate along the longitudinal axis of the polymer, presumably by π–π interactions between the styrene and vinyl end groups. Side-by-side van der Waals interactions between the polymer chains may lead to aggregation in the second dimension (Fig. 2d).

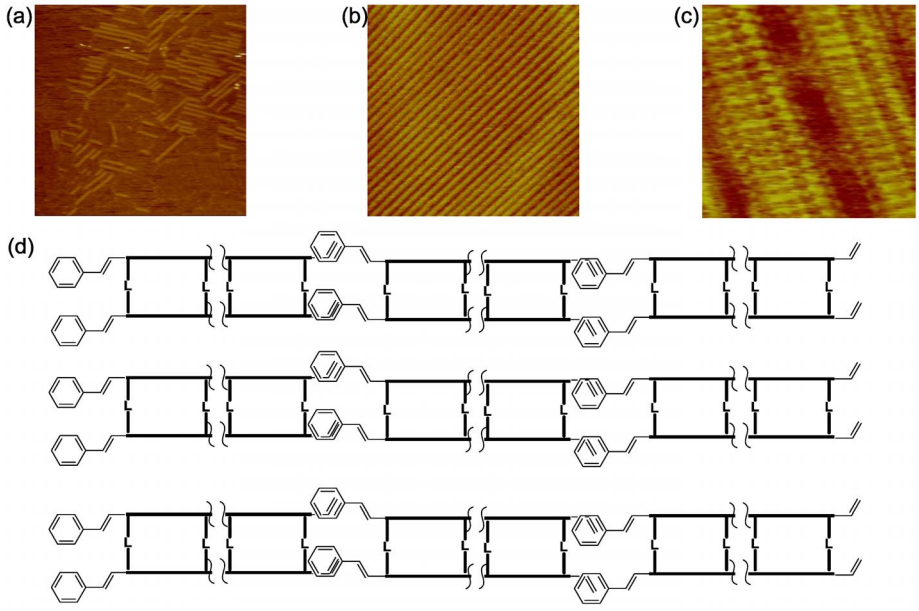

Fig. 2 STM images of **7** (a) at 100 nM; (b) 300 nM in phenyloctane (dimension 100 × 100 nm); (c) high-resolution image of **7**. (d) A cartoon to mimick the aggregation pattern via π–π interactions along longitudinal axis of the polymer and van der Waal interactions between polymer chains.

The scanning tunneling microscopic (STM) image of **10** (Fig. 2) obtained by the diimide reduction of **9** (Scheme 3) shows breakpoints along the longitudinal axis of the polymers [15]. Since all double bonds on the polymeric backbones in **9** are reduced, the end groups become the ethyl and phenylethyl moieties. As such, no more π–π interactions between the end groups in **10** will take place. The STM images of **10** shows that side-by-side van der Waals interactions between polymer chains hold the molecules in aggregation form. Lack of interactions between the end groups in **10** may account for the presence of the breakpoints along the longitudinal axis of the polymer [15].

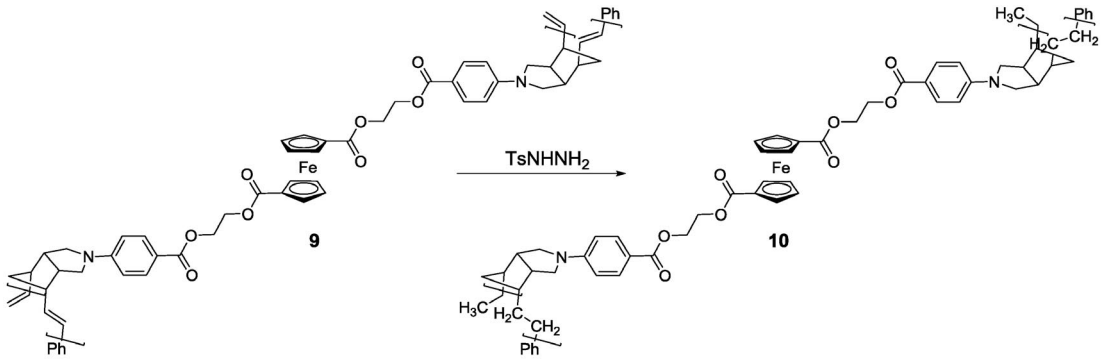

Scheme 3

DOUBLE-STRANDED LADDERPHANES WITH PLANAR AROMATIC LINKERS

As mentioned above, the span for each of the monomeric norbornene units in **2** and **7** is 5–6 Å. Any linker with a dimension (or thickness) less than this distance can properly fit into this space for the synthesis of these polynorbornene-based ladderphanes. Although the gap is somewhat larger than that expected for typical π–π stacking, planar aromatic species can certainly be the choice to be accommodated as the linker in ladderphanes. Indeed, Fig. 3 summarizes the representative double-stranded ladderphanes **11** that have recently been synthesized. The linkers can be simple oligoaryls (**11a–d**) [1], hexa-*peri*-hexabenzocoronene (HBC) derivatives (**11e**) [16], and even metalloporphyrin moiety (**11f**) [1]. Like ferrocene-incorporated ladderphanes **2** and **7** (Fig. 4), ladderphanes **11** also assemble nicely on the HOPG surface to form a highly ordered pattern. Representative examples are shown in Fig. 4.

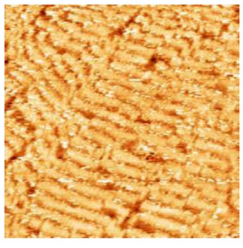

Fig. 3 STM image of **10**.

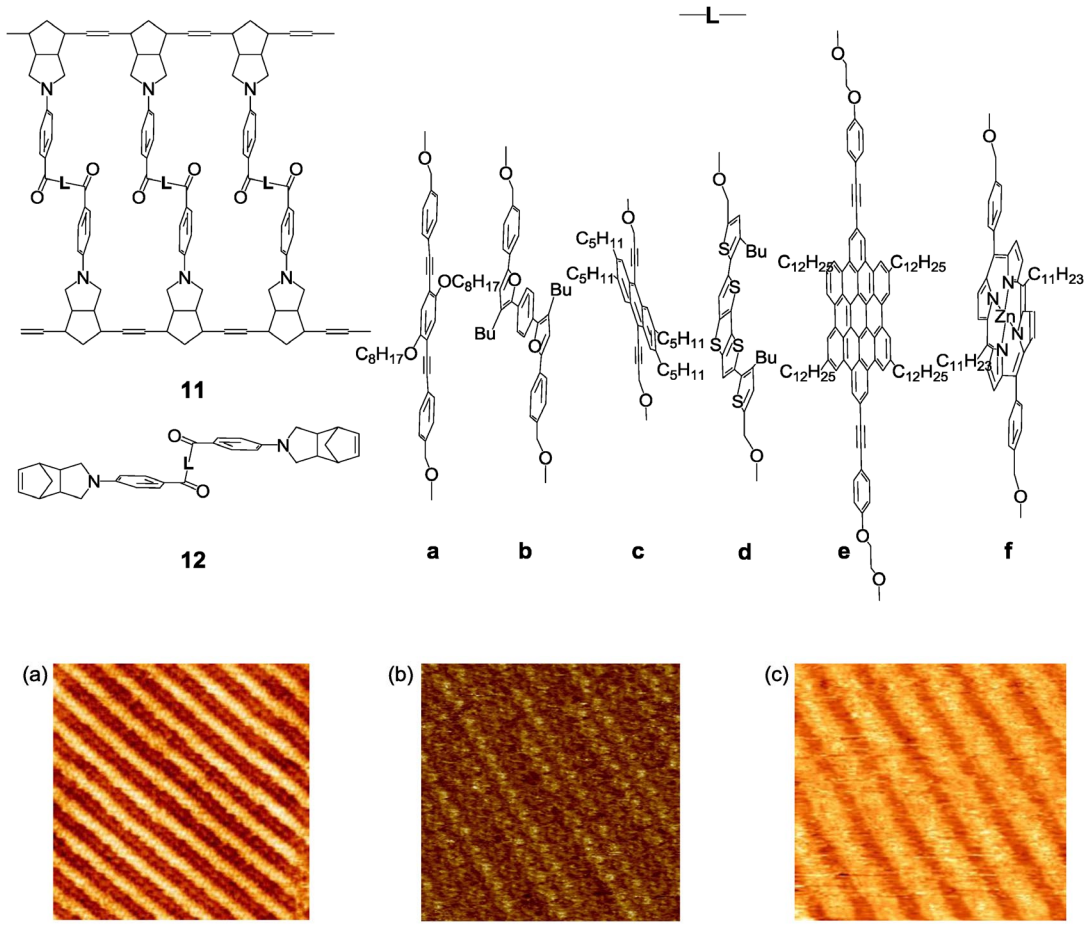

Fig. 4 STM images of (a) **11d** (45 × 45 nm), (b) **11b** (15 × 15 nm), and **11e** (22 × 22 nm) on HOPG.

Strong intereactions between adjacent linkers have been revealed by their photophysical properties in these polymers. Representative emission and absorption spectra are shown in Fig. 5. For example, the intensity of the emission profile of **11c** is much lower than that of the corresponding monomer **12c** (Fig. 5a) [1]. Excimer emission is found with polymeric ladderphane **11a** [1]. In addition, exciton coupling between porphyrin linkers is also observed with significant broadening of the Soret band in the absorption spectrum of **11f** in comparison with that of **12f** [1,17].

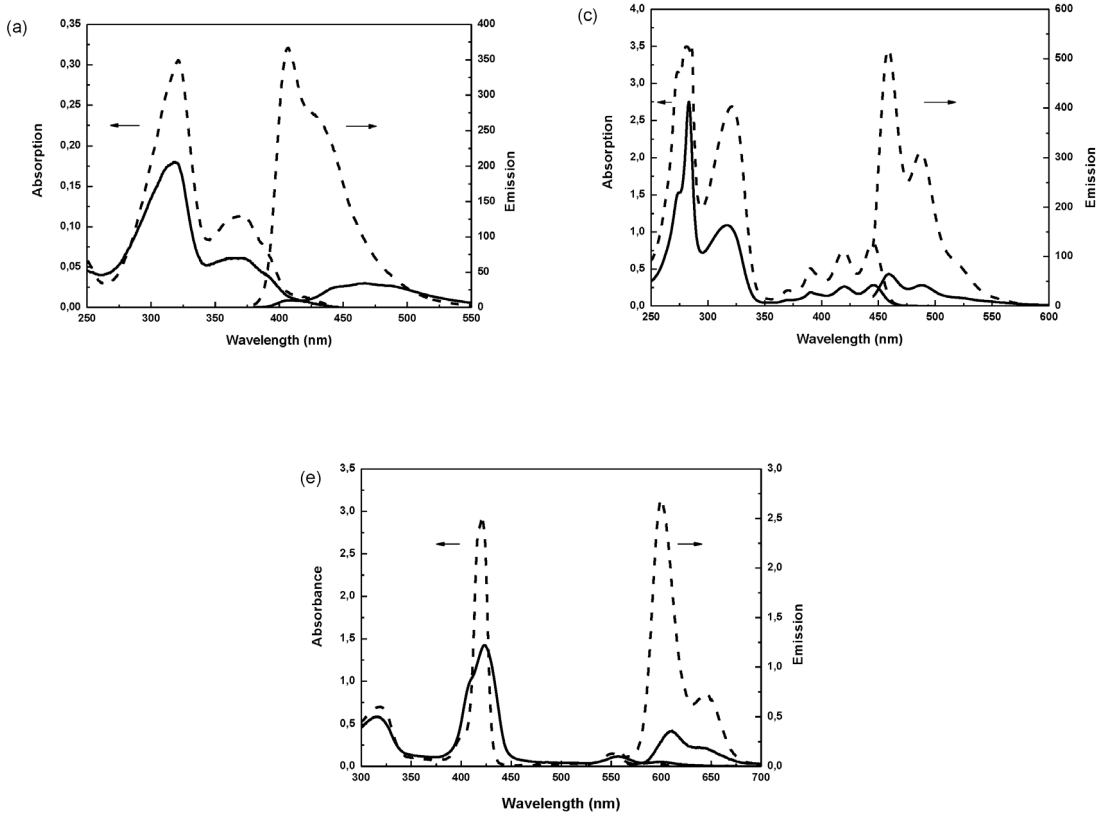

Fig. 5 Absorption and emission spectra (solid line for **11** and dashed line for **12**) of (a) **11a** and **12a**, (b) **11c** and **12c**, and (c) **11f** and **12f**.

TRIPLE-STRANDED LADDERPHANES

Triple-stranded polymeric ladderphanes **13** with multilayer planar oligoaryl linkers having C_3 symmetry are synthesized by G-I catalyst-mediated ring-opening metathesis of tris-norbornene derivatives **14**. All linkers are coherently aligned perpendicular to the longitudinal axis of the polymer. Interactions between these linkers lead to fluorescence quenching or perturbation of frontier orbitals resulting in shift of the emission maximum. These triple-stranded polymeric ladderphanes tend to self-assemble to

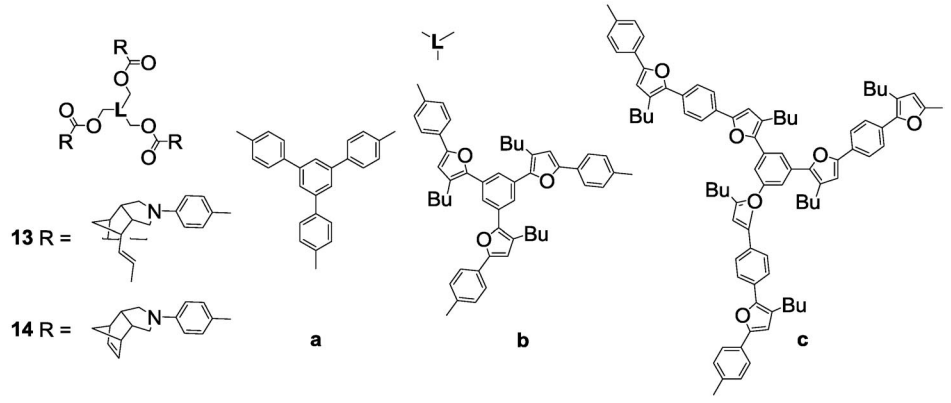

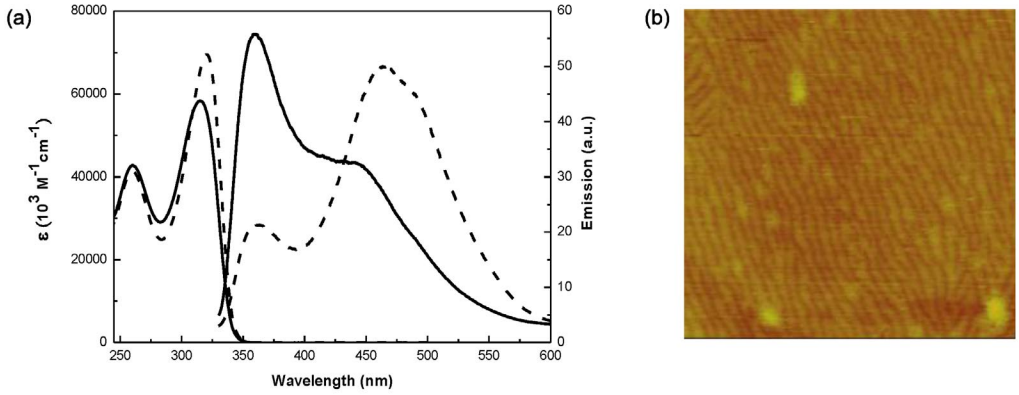

Fig. 6 (a) Absorption and emission profiles of **13a** (solid) and **14a** (dash). (b) TMAFM image of **13b** on HOPG (300 × 300 nm).

form an ordered pattern as revealed by tapping-mode atomic force microscopy (TMAFM) [18]. The representative spectra of **13a** and **14a** and the TMAFM image of **13a** are shown in Fig. 6.

HELICAL POLYMERIC LADDERPHANES

Incorporation of asymmetric centers in the linker has been demonstrated to induce helicity of the double-stranded ladderphanes. Thus, helical polymeric ladderphanes with C_2-chiral ferrocene linkers **15** are synthesized from the corresponding monomers. As shown in Fig. 7, the enantiomeric pairs of **15-*M*** and **15-*P*** exhibit mirror-imaged circular dichroic (CD) profiles in the UV region (250–360 nm) and the CD properties are significantly enhanced in comparison with those of the corresponding monomers **16**. Exciton coupling between adjacent aminobenzoate groups would be responsible for the CD enhancement. It is worth noting that when the phenyl substituents in **15** are replaced by alkyl groups, the CD curves appear only as a hump [7]. The STM images of both enantiomers **15-*M*** and **15-*P*** on HOPG clearly exhibit the supercoil structures (Fig. 8). The aggregated form of **15-*M*** is also shown in Fig. 8c [7].

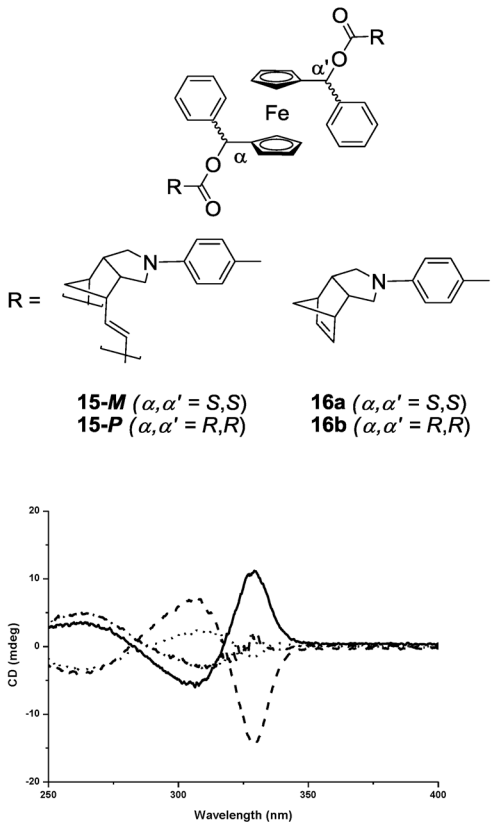

Fig. 7 CD curves of **15-*P*** (solid), **15-*M*** (dash), **16a** (dash–dot), and **16b** (dot).

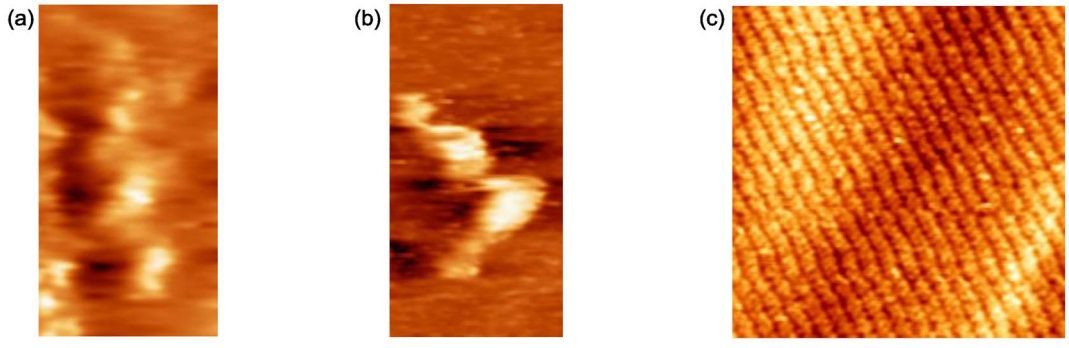

Fig. 8 STM image of (a) **15-*P*** (10 × 20 nm), (b) **15-*M*** (10 × 20 nm), and aggregation patter of **15-*M*** (80 × 80 nm) on HOPG.

CHEMICAL REACTIONS OF LADDERPHANES

Ferrocene is redox active. A redox peak pair around 100 mV (with reference to ferrocene/ferrocenium couple) corresponds to the redox of ferrocene moieties in **1**. Thus, oxidation of the ferrocene moieties in **15** and related polymers are examined by the chronoamperometric method [19] at a microelectrode or by bulk-electrolysis experiments. On the average, about 70 % of the total ferrocene units in **15** and related polymers are electrochemically oxidized during a potential-step process [11]. The oxidized **15**

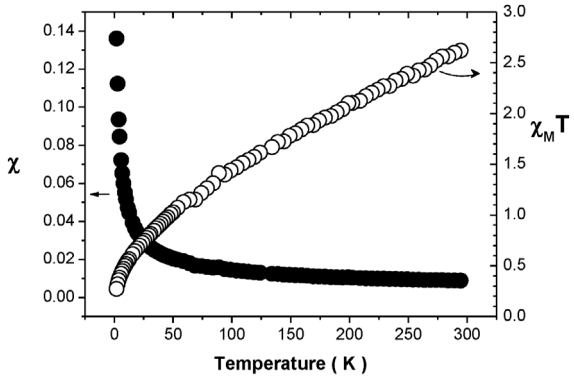

Fig. 9 Magnetic susceptibility of the oxidized **15** as a function of temperature. The solid (χ) and open circle ($\chi_M T$) are experimental data based on 10 monomeric units after correction on diamagnetism and normalization on the applied magnetic field.

was subjected to magnetic susceptibility (χ) measurements (Fig. 9) and has been shown to exhibit antiferromagnetic property. These results indicate that the each of neighboring monomeric units in **15** may couple with each other, and, on the average, two holes are generated among every three ferrocene-containing monomeric units [11].

The polynorbornene-based double-stranded ladderphanes have double bonds on the polymeric backbones. Besides diimide reduction mentioned above (from **9** to **10**) resulting in totally reduced product [15], double bonds in these polymers can also be dihydroxylated to give the corresponding polyols. Thus, **17** was allowed to react with OsO_4 under Narasaka conditions ($NMO/OsO_4/PhB(OH)_2/DCM$) [20]. The slow addition protocol [21] was employed to give the corresponding phenylboronic ester, which was transesterified into **18** (Scheme 4) [22].

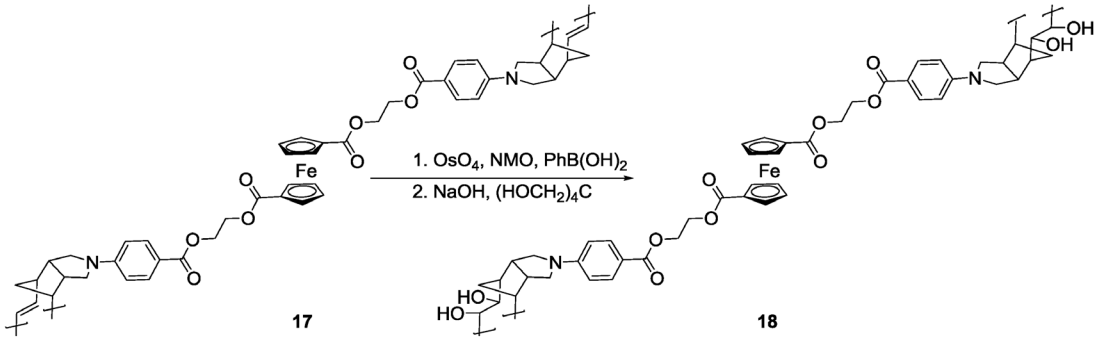

Scheme 4

The STM image on the highly oriented pyrolytic graphite (HOPG) surface is shown in Fig. 10. It is interesting to note that polymers with equal lengths tend to form aggregate. Presumably, full usage of all available hydroxyl groups on the polymeric backbones for hydrogen bonding may be responsible for such alignment [22]. It is interesting to note that **18** in the aggregate are assembled in staggered form along the longitudinal direction. Presumably, the hydrogen bonding may also be formed between the terminal diols and the carbonyl group in the ester linkers as shown in Fig. 10b.

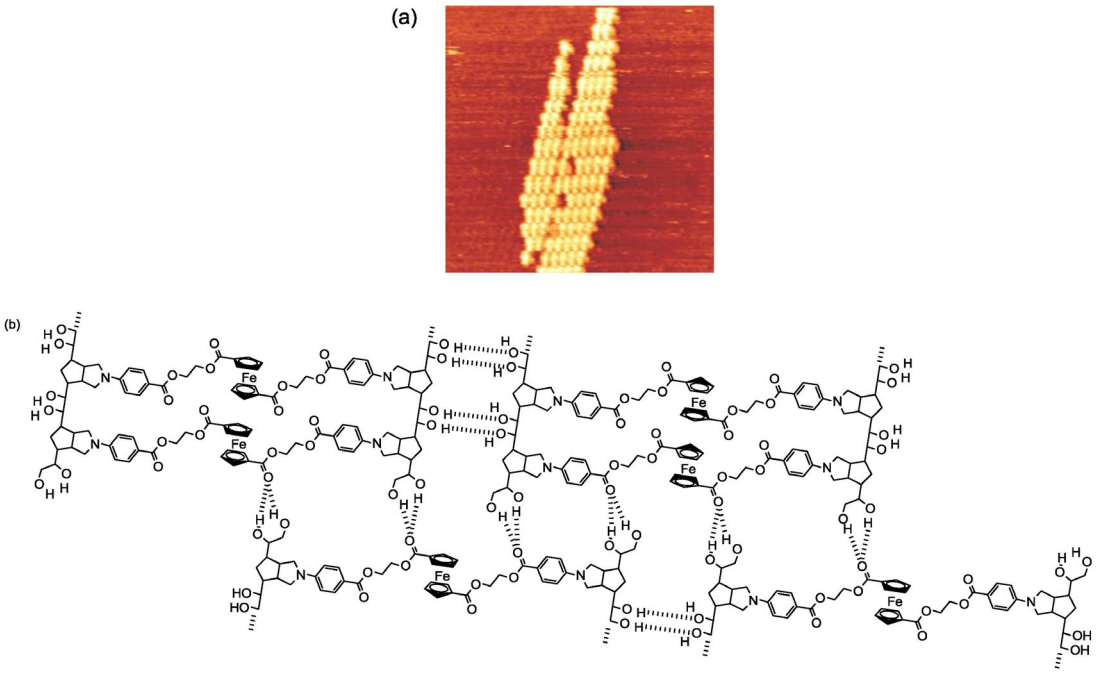

Fig. 10 (a) STM image of **18** on HOPG (108 × 108 nm). (b) Schematic representation of the assembly of **18** by hydrogen bonding.

UNSYMMETRIC LADDERPHANES BY SEQUENTIAL POLYMERIZATION

DNA molecules are unsymmetrical complementary double-stranded ladderphanes. As shown in eq. 2, single-stranded polynorbornene **4** can serve as the template to obtain the corresponding complementary polynorbornene **8** via unsymmetric ladderphane **7** by the reaction sequence shown in eq. 2 [14]. This protocol can be considered to be analogous to the replication in DNA chemistry. Another approach toward an unsymmetrical double-stranded ladderphane involves sequential polymerizations of a monomer containing two different polymerizable groups which can undergo polymerization under different reaction conditions. Thus, polymerization of **19** in the presence of the G-I catalyst afforded the corresponding diethynyl benzene appended polynorbornenes **20**. Since ROMP of a cycloalkene catalyzed by the G-I catalyst is a living polymerization [23], polymers **20** of different degrees of polymerization are obtained when different amounts of G-I catalyst are used. Further Glaser oxidation of **20** gives the corresponding unsymmetrical polymeric ladderphanes **21** in 76–80 % yields. Hydrolysis of **21** with NaOH yields **22** in 74–77 % yields. This protocol offers a general route for the selective synthesis of poly(arylene-butadiynylene) **22** with narrow polydispersity index (PDI) and controlled chain lengths. The strategy in general provides a new entry for template synthesis of polymers with well-defined chain length and narrow polydispersity [24].

As shown in Fig. 11a, **21** shows absorptions due to the aminobenzoate (320 nm) and the substituted diarylbutadiyne chromophores. The emission of **21** in CH_2Cl_2 exhibits, in addition to the intrinsic emission attributed to the substituted poly(*m*-arylene-butadiynylene) **22** at 391 nm, a broad charge-transfer band around 478 nm (Fig. 11b). It is known that an aminobenzoate moiety like that in **19** exhibits typical charge-transfer emission at 460 nm. This emission was shifted to shorter wavelength at 434 nm in **20** arising from interactions between the adjacent chromophores, which is typical in related aminobenzoate-appended polynorbornenes [6–18].

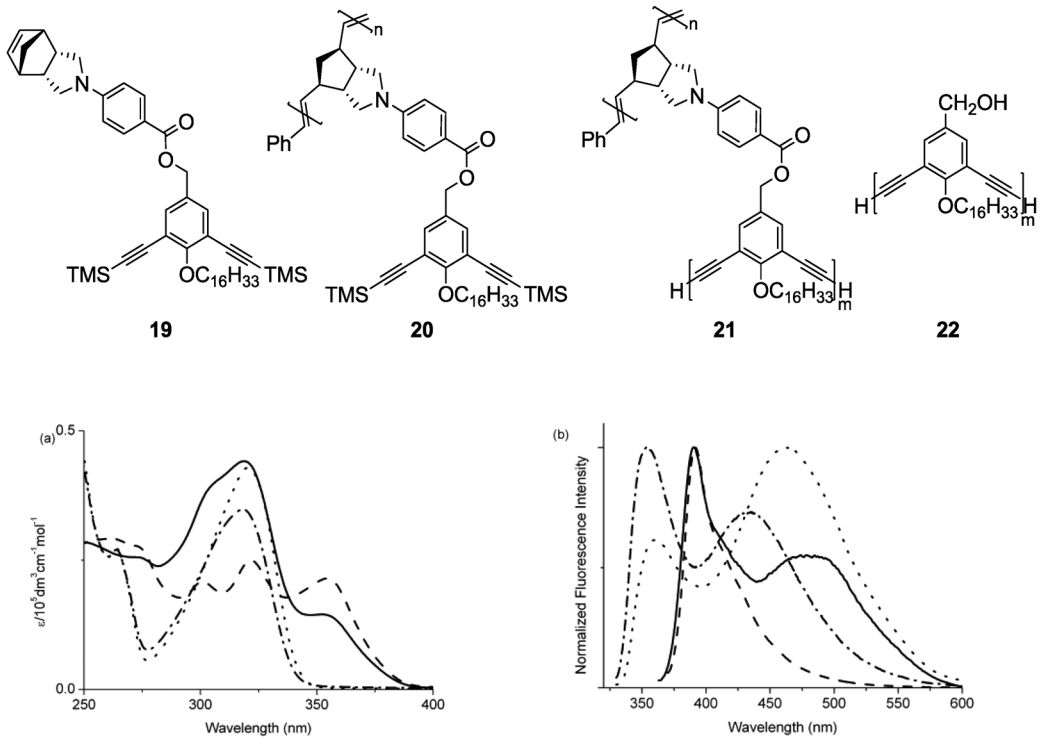

Fig. 11 (a) Absorption and (b) emission spectra of **19** (dot, λ_{ex} = 320 nm), **20** (dash–dot, λ_{ex} = 318 nm), **21** (solid, λ_{ex} = 354 nm), and **22** (dash, λ_{ex} = 355 nm) in CH_2Cl_2.

Like polynorbornene-based ladderphanes described above [1,6,15,16,18], **21** also exhibits self-assembled ordered images on HOPG. As shown in Fig. 12, the left side of each of the polymeric stripes appears brighter than the right side of the stripes. Presumably, the conjugated oligomeric diarylbutadiyne moieties in **21** would have better contact with the graphite surface resulting in brighter images, whereas the polynorbornene moieties in **9** may show dimmer images. As described above, **21** may be considered as a linear array of the donor–acceptor pairs along the polymeric backbones. The morphology shown in Fig. 12 is consistent with this property, and it seems likely that the donor and acceptor arrays are arranged in an alternative manner on the HOPG surface [24].

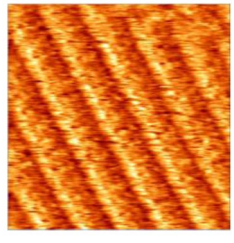

Fig. 12 STM image of **21** on HOPG (22 × 22 nm).

CONCLUSIONS

We have summarized our recent studies on the design, synthesis, characterization, photophysical properties, and morphology of a range of different double-stranded polymeric ladderphanes. The unique rod-like structural features, no matter whether they are symmetrical or unsymmetrical ladderphanes, can be demonstrated by the assembly on HOPG surface. Interactions between end groups (styryl and vinyl) along the longitudinal axes of polymers and van der Waals force between adjacent polymers would be responsible for these highly order patterns. Interactions between linkers in these polymers, which are separated by 5–6 Å, are revealed by photophysical and electrochemical properties and the STM images. These supramolecular architectures offer a possibility to assemble various planar π-systems cofacially for materials applications.

ACKNOWLEDGMENTS

We thank the National Science Council and the National Taiwan University for support. Thanks are also due to co-workers whose names are listed in the references for their invaluable contributions.

REFERENCES AND NOTES

1. C.-M. Chou, S.-L. Lee, C.-H. Chen, A. T. Biju, H.-W. Wang, Y.-L. Wu, G.-F. Zhang, K.-W. Yang, T.-S. Lim, M.-J. Huang, P.-Y. Tsai, K.-C. Lin, S.-L. Huang, C.-h. Chen, T.-Y. Luh. *J. Am. Chem. Soc.* **131**, 12579 (2009).
2. H. E. Katz, Z. Bao, S. L. Gilat. *Acc. Chem. Res.* **34**, 359 (2001).
3. F. Würthner. *Angew. Chem., Int. Ed.* **40**, 1037 (2001).
4. M. Bendikov, F. Wudl, D. F. Perepichka. *Chem. Rev.* **104**, 4891 (2004).
5. J. E. Anthony. *Chem. Rev.* **106**, 5028 (2006).
6. H.-C. Yang, S.-Y. Lin, H.-c. Yang, C.-L. Lin, L. Tsai, S.-L. Huang, I.-W. P. Chen, C.-h. Chen, B.-Y. Jin, T.-Y. Luh. *Angew. Chem., Int. Ed.* **45**, 726 (2006).
7. H.-C. Yang, S.-L. Lee, C.-h. Chen, N.-T. Lin, H.-C. Yang, B.-Y. Jin, T.-Y. Luh. *Chem. Commun.* 6158 (2008).
8. For a review, see: T.-Y. Luh, H.-C. Yang, N.-T. Lin, S.-Y. Lin, S.-L. Lee, C.-h. Chen. *Pure Appl. Chem*. **80**, 819 (2008).
9. W.-Y. Lin, M. G. Murugesh, S. Sudhakar, H.-C. Yang, H.-C. Tai, C.-S. Chang, Y.-H. Liu, Y. Wang, Y. I.-W. P. Chen, C.-h. Chen, T.-Y. Luh. *Chem.—Eur. J.* **12**, 324 (2006).
10. W.-Y. Lin, H.-W. Wang, Z.-C. Liu, J. Xu, C.-W. Chen, Y.-C. Yang, S.-L. Huang, H.-C. Yang, T.-Y. Luh. *Chem. Asian J.* **2**, 764 (2007).
11. C.-L. Lin, H.-C. Yang, N.-T. Lin, I.-J. Hsu, Y. Wang, T.-Y. Luh. *Chem. Commun.* 4484 (2008).
12. H.-W. Wang, Z.-C. Liu, C.-H. Chen, T.-S. Lim, W. Fann, C.-G. Chao, J.-Y. Yu, S.-L. Lee, C.-h. Chen, S.-L. Huang, T.-Y. Luh. *Chem.—Eur. J.* **15**, 5719 (2009).
13. J. A. Sattigeri, C.-W. Shiau, C.-C. Hsu, F. F. Yeh, S. Liou, J.-B. Jin, T.-Y. Luh. *J. Am. Chem. Soc.* **121**, 1607 (1999).
14. N.-T. Lin, S.-Y. Lin, S.-L Lee, C.-h. Chen, C.-H. Hsu, L.-P. Hwang, Z.-Y. Xie, C.-H. Chen, S.-L. Huang, T.-Y. Luh. *Angew. Chem., Int. Ed.* **46**, 4481 (2007).
15. S.-L. Lee, N.-T. Lin, W.-C. Liao, C.-h. Chen, H.-C. Yang, T.-Y. Luh. *Chem.—Eur. J.* **15**, 11594 (2009).
16. C.-W. Chen, H.-Y. Chang, S. L. Lee, I.-J. Hsu, J.-J. Lee, C.-h. Chen, T.-Y. Luh. *Macromolecules* **43**, 8741 (2010).
17. H.-W. Wang, C.-H. Chen, T.-S. Lim, S.-L. Huang, T.-Y. Luh. *Chem. Asian J.* **6**, 524 (2011).
18. K.-W. Yang, J. Xu, C.-H. Chen, H.-H. Huang, T. J.-Y. Yu, T.-S. Lim, C.-h. Chen, T.-Y. Luh. *Macromolecules* **43**, 5188 (2010).

19. G. Denuault, M. V. Mirkin, A. J. Bard. *J. Electroanal. Chem.* **308**, 27 (1992).
20. H. Sakurai, N. Iwasawa, K. Narasaka. *Bull. Chem. Soc. Jpn.* **69**, 2585 (1996).
21. J. S. M. Wai, I. Marko, J. S. Svendsen, M. G. Finn, E. N. Jacobsen, K. B. Sharpless. *J. Am. Chem. Soc*. **111**, 1123 (1989).
22. N.-T. Lin, S.-L. Lee, J.-Y. Yu, C.-h. Chen, S.-L. Huang, T.-Y. Luh. *Macromolecules* **42**, 6986 (2009).
23. R. H. Grubbs (Ed.). *Handbook of Metathesis*, Vols. 1–3, Wiley-VCH: Weinheim (2003).
24. Y.-Z. Ke, S. L. Lee, C.-h. Chen, T.-Y. Luh. *Chem. Asian J.* **6**, 1748 (2011).

